

## Calendered Linear Low-Density Polyethylene Consolidated Meat and Bone Meal Composites

Sam Lukubira, Amod Ogale

Department of Chemical and Biomolecular Engineering, and Center for Advanced Engineering Fibers and Films, Clemson University, Clemson, South Carolina 29634

Correspondence to: A. Ogale (E-mail: ogale@clemson.edu)

**ABSTRACT:** Bioplastics produced from meat and bone meal (MBM) suffer from rapid and drastic mechanical property deterioration because of their hydrophilic nature. This study investigates mechanical and water stability of composites produced from introduction of a minor component of a synthetic polyethylene as a binder phase to consolidate MBM. The milled and sieved MBM was compounded with 5–60 wt % linear low-density polyethylene (LLDPE) and formed into composite sheets by calendering, which is an industrially relevant process. Results indicated that a minimum of 15 wt % LLDPE content was required to form a nominally continuous binder phase that allowed for good processability and environment stability of the composites. As expected, the water vapor permeability (WVP) and water absorption characteristics of the composites were intermediate between those of MBM and LLDPE. Sheets containing 15 wt % LLDPE absorbed up to 35 wt % water. Composites tested after being soaked in water showed an initial decrease in TS of about 30% for the first hour but then remained fairly unchanged in the next 72 hours, confirming their moderate environment stability. © 2014 Wiley Periodicals, Inc. *J. Appl. Polym. Sci.* **2014**, *131*, 41145.

**KEYWORDS:** biopolymers & renewable polymers; composites; differential scanning calorimetry (DSC); polyolefins; structure-property relations

Received 16 March 2014; accepted 11 June 2014

DOI: 10.1002/app.41145

### INTRODUCTION

Meat and bone meal (MBM) is an animal co-product that is derived from the rendering of animal parts not utilized for food by humans and is typically used as animal feed.<sup>1,2</sup> It has become available for alternative uses because of increased regulations restricting its feed applications due to its association with bovine spongiform encephalopathy disease.<sup>1,2</sup> MBM has been shown to be thermally processable into plastic-like sheets when modified with low molecular weight plasticizers (e.g., glycerol).<sup>3</sup> However, such hydrophilic plasticizers also increase moisture susceptibility of the MBM sheets, and lead to rapid deterioration of the mechanical properties with increasing environmental humidity.<sup>3–5</sup>

A strategy to prevent this performance deterioration and enhance mechanical properties is the use of synthetic polymers as binders during the processing of bioplastic sheets, to produce MBM-polymer composites (MBMPCs) with MBM as the major content (>50 wt %). Synthetic polymers [e.g., linear low-density polyethylene (LLDPE)] have excellent mechanical and barrier properties and are easy to process.<sup>6,7</sup> However, they are derived from fossils and are non-biodegradable.<sup>6</sup> MBMPCs are attractive because they can easily be integrated with industrial

polymer processing routes, and can reduce the content of synthetic polymers, which addresses sustainability concerns associated with the use of petroleum-based plastics. Thus, composites consisting of renewable biomaterial particulates and synthetic polymers are of topical interest from an environmental sustainability perspective.<sup>8–11</sup>

Composites such as particle boards, where the particulates make up more than 50 wt % of the composite, have been investigated in literature studies.<sup>10–12</sup> The particulates are mainly cellulosic materials, e.g., wood flour, wheat stalk, sugar cane bagasse, and cornhusks.<sup>10–12</sup> The adhesives/binders used for such composites are mainly thermosetting resins that include urea-formaldehyde, phenol formaldehyde, melamine formaldehyde, and diphenyl diisocyanate.<sup>13</sup> However, use of such thermosets possess a risk of potential harmful formaldehyde emissions, limited recyclability and processing.<sup>13</sup>

Other bio-particulates of non-cellulosic origin such as egg shells, chicken feathers, sea weed, and waste shell fish have been incorporated as fillers into synthetic polymers at fractions usually <30 wt %.<sup>8,14–16</sup> Studies have been conducted with a low concentration of MBM as a filler in high-density polyethylene.<sup>17</sup> However, studies on processing large weight fractions of MBM



**Figure 1.** Calendering of MBMPC sheet containing 15 wt % LLDPE using the Collin calender roll. [Color figure can be viewed in the online issue, which is available at [wileyonlinelibrary.com](http://wileyonlinelibrary.com).]

with synthetic polymers using conventional thermoplastic processing routes such as calendering, which an industrially relevant process, have not been reported in literature. Therefore, MBM particulates were consolidated using a thermoplastic LLDPE as the minor phase. Specific objectives of this research were to: (i) study the microstructure of MBMPCs as a function of different MBM contents for sheets produced by calendering and (ii) characterize the improvement of moisture resistance and resulting mechanical properties of the bio-based composites. While not a strategy that completely eliminates synthetic polymers, the one discussed here minimizes synthetic content significantly and adds value to MBM material. Note also that inorganic fillers like calcium carbonates, talc/clays and carbon black, which are used as plastic fillers, cannot be used as processing aides for MBM because they cannot encapsulate it.<sup>18–20</sup>

## EXPERIMENTAL

### Materials

MBM (Darling International, Inc.) was used throughout this study. It is a rendered animal co-product with an approximate composition of 50 wt % protein, 8–12 wt % fat, 4–7 wt % moisture, and 35 wt % ash according to the manufacturer. Because as-received MBM contains large bone particles, it was milled and sieved through a 60 mesh sieve (250  $\mu\text{m}$  opening) to obtain a bottom product that was used in further processing. LLDPE (Dowlex 2045 LLDPE) with a melt flow index (MFI at 190°C/2.16 kg) of 1.0 g/min and density of 0.92 g/cc (Dow chemical company) was used throughout the study.

### Processing MBM-Polyethylene Composites

Milled and sieved MBM was intensively blended with 5, 10, 15, 30, 40, and 60 wt % LLDPE using a Haake Rheomix 600 batch mixer at 140°C for 15 mins and 60 rpm mixing speed. The different mixed compositions of MBM-LLDPE were formed into MBMPC sheets using a Collin calender roll mill (model W 100T) with two counter-rotating rolls. Calendering was conducted at 135°C and 3–15 rpm with the gap between the rolls set to 0.25 mm as shown in Figure 1; the illustrated calendered sheet is about 10 cm wide.

### Thermal Analysis and Scanning Electron Microscopy (SEM)

Differential scanning calorimetry (DSC) analyses of the composites were performed using a Perkin-Elmer Pyris DSC from 30 to 145°C at 10°C/min in nitrogen atmosphere. Each sample was exposed to two heating and two cooling scans. Prior to DSC, thermal gravimetric analyses were conducted at a heating rate of 10°C/min from 30°C to 500°C. However, those results were not included in the paper because DSC provided the relevant information on processing of MBMPCs.

SEM (SEM-Hitachi S4800) was used to analyze the microstructure of cryogenically fractured cross-section surfaces of the calendered MBMPCs.

### Tensile and Flexural Properties

Tensile tests were conducted following the ASTM D638-10 procedure using dog-bone specimen (type V) die-cut from the calendered sheets both in the longitudinal and transverse direction. Mechanical testing of the sheets was performed at a cross-head speed of 0.25 cm/min (Applied Test Systems Inc., Series 900). The flexural modulus (FM) was obtained from three point dynamic strain sweep using RSA 3 TA Instruments rheometer at 25°C, 0.002% strain and 6.28 rad/s frequency. The test specimens were nominally 2 mm thick, 12.5 mm wide, and 50 mm in length. The three point bend fixture used had a span of 40 mm. A minimum of four replicates for each composition were tested. Samples of MBMPCs were conditioned at 50% RH and 25°C for 48 hours. Analysis showed that there was no significant difference in tensile properties for specimen tested either in longitudinal or transverse direction. Therefore, results presented herein are for longitudinally cut specimen. In addition, tensile tests on samples of MBMPCs containing 10, 15, and 30 wt % LLDPE were performed on specimen soaked in water for 1 and 3 days.

### Water Vapor Permeability (WVP) and Water Absorption

The tests were carried out following the ASTM E 96-05 [Standard Test Methods for Water Vapor Transmission (WVT) of Materials]. Two replicate circular discs, each having an area of 28.3 cm<sup>2</sup>, were placed on the testing cups each containing 15 mL of distilled water. The cups were tightened by screws, leaving an exposed area of 19.6 cm<sup>2</sup>. The cups were placed in the WVP testing chamber (Model 506A Electro-tech Systems Inc.) maintained at controlled relative humidity (RH) and temperature. Within the chamber, a Denver instrument Model # P-603-D balance was used to obtain mass as a function of time.

The temperature and humidity were stabilized for 24 hours before testing began. Measurements were taken at 1 hour intervals for the first 12 hours, and then every 5 hours. From a linear regression of the mass versus time curve, WVT in g/m<sup>2</sup>/s was calculated as:  $WVT = (\text{slope}/\text{Area}) \times 1 \text{ hr}/3600 \text{ s}$

Then, WVP in g/m.s.Pa, was calculated as:

$WVP = [(WVT) \times T]/SVP (RH_1 - RH_2)$ , where SVP = saturation vapor pressure (Pa) =  $3.166 \times 10^3$  at 25°C, T (m) = average thickness of the test specimen, RH<sub>1</sub> = relative humidity in the test cup  $\approx$  100%, RH<sub>2</sub> = relative humidity of the chamber = 50%.

The water absorption of calendered MBMPC sheets was determined by using circular discs of 2 mm thickness and 25 mm

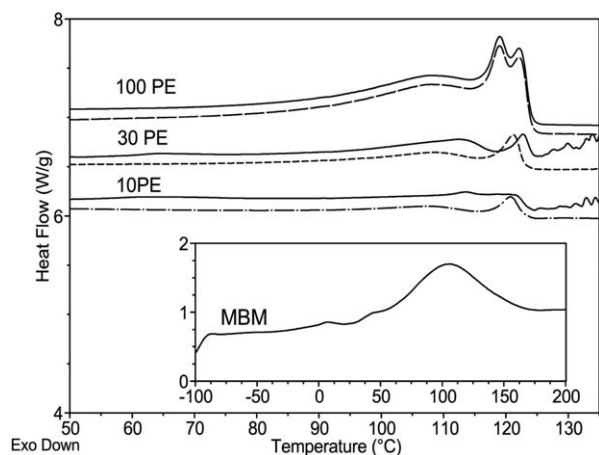


**Figure 2.** First and second heating DSC thermograms of MBMPCs containing 10 wt % and 30 wt % LLDPE (PE) compared to pure LLDPE. The first heating is indicated by continuous lines while the second heating is represented by discontinuous lines. The inset displays a thermogram of MBM powder showing a large endotherm between 50 and 200°C and other transitions.

diameter. Three specimen of each composition were initially dried in a vacuum oven ( $\sim 100$  kPa vacuum) at 50°C for 48 hours. The specimens were then placed in separate glass beakers filled with distilled water (200 mL). The samples were withdrawn at intervals of 2 hours for the first 10 hours and less frequently thereafter to record their mass gain. The samples were lightly wiped with a paper towel to remove surface water before being weighed. The mass of the samples were recorded for up to 72 hours.

## RESULTS AND DISCUSSION

### DSC Analysis of MBMPCs

Figure 2 displays the first and second heating thermograms of MBMPCs containing 10 and 30 wt % LLDPE compared to pure LLDPE. It is observed that both the first and second heating thermograms of LLDPE are similar and have a flat baseline after the melting peaks. In contrast, those of the composites are variable, with the first heating baselines being wavy after 125°C. This is an indication of the thermal sensitivity of composites containing biomass (MBM) in the given temperature range. The first heating thermograms of composites containing 10 wt % LLDPE do not display a sharp endothermic peak, although there is a broad endotherm from about 60 to 125°C. When the ratio of MBM to LLDPE in the composite is reduced from 9 (10 wt % PE) to 2.3 (30 wt % PE), two endothermic peaks are observed in addition to the broad endotherm. The observed broad endotherm, and the characteristic difference of MBMPC thermograms from the first heating thermograms, is due to water evaporation and protein denaturation in combination with LLDPE melting.

Previous DSC studies on thermal processing of MBM have shown that it displays a broad endothermic peak between 50 and 200°C (Figure 2 inset) despite prior thermal treatments. The endotherm has been observed in other protein studies and is related to water loss and protein denaturation (unfolding).<sup>3,21,22</sup>

Therefore, because of these endothermic events, the sharp melting transitions of LLDPE in the first heating are masked. However, once the composites were reheated to 145°C, the protein transitions disappeared and the second thermograms displayed sharp melting peaks between 108 and 122°C with flat baselines. The irreversibility of protein transitions in DSC measurements may be attributed to complete denaturation of most of the ordered secondary structures that are part of the molten globule state (compact intermediate conformation) proteins formed during prior thermal treatments.<sup>23</sup> Therefore, compounding and calendaring of MBMPCs was done at temperatures ranging between 135 and 150°C that are sufficiently above melting of the LLDPE phase (122°C) but well below 200°C, where significant MBM decomposition is observed.<sup>3</sup>

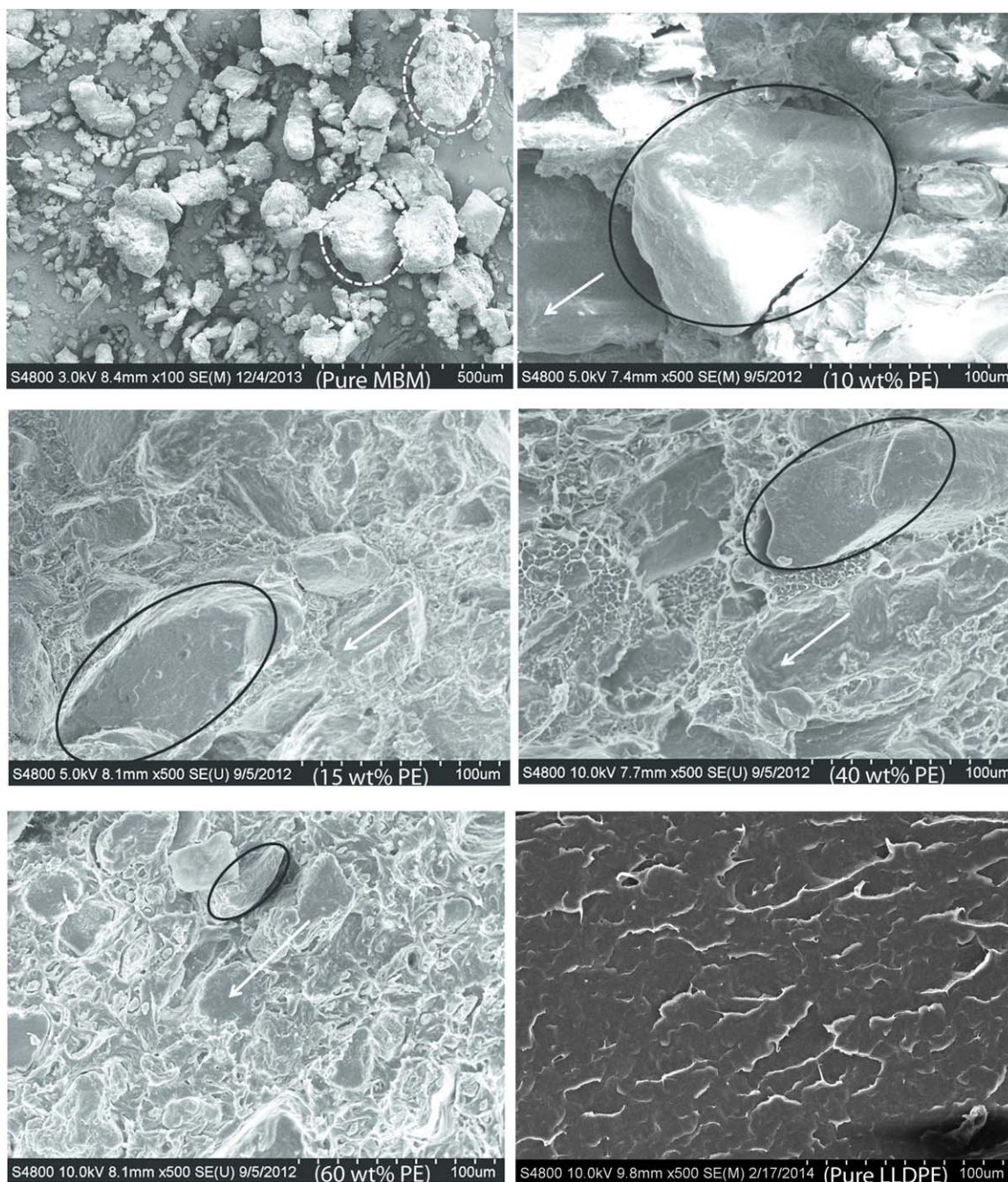
### Microstructure

Figure 3 displays SEM micrographs of cryogenically fractured cross-sections of pure LLDPE and MBMPCs containing different LLDPE contents; MBM powder is also shown for comparison. The representative MBM micrograph displays a wide range of particle sizes ranging from  $\sim 10$  to 200  $\mu\text{m}$  (some highlighted within dashed circles) nominal diameter. In the MBMPC micrographs, the lighter phase is the LLDPE matrix, whereas MBM shows up as dark irregular agglomerates (some highlighted within circles) varying from  $\sim 100$   $\mu\text{m}$  down to  $< 1$   $\mu\text{m}$ . Generally, it was observed that the MBM agglomerates reduced in size as the polyethylene content in the composites was increased. At 10 wt % LLDPE content, the MBM particles were barely encapsulated by the polyethylene, and large MBM particles ( $> 100$   $\mu\text{m}$ ) appear to touch one another. At 15 wt % LLDPE content, large agglomerates were still observed although the MBM particles appear to be surrounded by LLDPE matrix. Increase in the LLDPE content to 40 wt % resulted in decrease of MBM agglomerate size, with the largest agglomerate being only about 60  $\mu\text{m}$  and the average agglomerate size about  $40 \pm 16$   $\mu\text{m}$ . At 60 wt % LLDPE, the average agglomerate size reduced further to  $25 \pm 9$   $\mu\text{m}$ .

Furthermore, the SEM micrographs revealed that there was a small preferential axial orientation (white arrows) of MBM agglomerates especially apparent in composites containing more than 10 wt % LLDPE content, as indicated by the slightly elongated shape. Particle orientation in the calendared composites occurs because of elongation deformation as the blend is nipped through the counter-rotating rolls.<sup>24</sup> Although textural orientation in the MBM phase was observed, the LLDPE phase did not show significant orientation, due to the low calendaring speed and the slow cooling that allowed molecular relaxation within the LLDPE phase.

The SEM images indicate that MBM exists as irregular agglomerates in the MBMPC sheets, because it is largely hydrophilic and incompatible with the hydrophobic LLDPE binder. This incompatibility results in phase separation similar to what has been observed in composites of starch and polyethylene.<sup>25</sup> However, when sufficient mechanical energy is transferred from LLDPE to MBM during mixing, shearing action causes the agglomerates to break down to smaller sizes.<sup>24</sup> These smaller domains are encapsulated by the polymer and are held tight on cooling because of the higher





**Figure 3.** Representative SEM micrographs of MBM composite sheets consolidated with different LLDPE content compared to pure LLDPE and pure MBM powder. The white arrows indicate the longitudinal axis of calendaring and the circles highlight some of the MBM particles. [Color figure can be viewed in the online issue, which is available at [wileyonlinelibrary.com](http://wileyonlinelibrary.com).]

thermal expansion coefficient of LLDPE ( $\sim 200 \times 10^{-6}/\text{K}$ ) consistent with literature studies on other polymer composites.<sup>7,13,25,26</sup> This underscores the importance of using LLDPE in MBMPCs processing rather than inorganic components like calcium carbonate, talc/clays and carbon black, which cannot encapsulate MBM.<sup>18–20</sup>

#### Mechanical Properties

For the various compositions of MBMPCs evaluated, the tensile strength (TS), strain-to-failure (STF), tensile modulus (TM), and

flexural modulus (FM) are summarized in Table I. The TS and STF of MBMPC sheets increased with increasing LLDPE content. The TS for 10 and 60 wt % LLDPE content ranged between  $0.7 \pm 0.1$  MPa and  $6.3 \pm 0.2$  MPa, and STF ranged from  $2.3 \pm 0.3$  to  $107.9 \pm 58.9\%$ . This behavior is consistent with particle-filled composites with poor adhesion between the particulates and polymer matrix.<sup>27</sup> The TS and STF of MBMPCs increased with increasing LLDPE content because it forms a continuous phase that has superior load-carrying properties relative to that of MBM.<sup>28</sup>

**Table I.** Summary of Tensile Strength (TS), Strain-to-Failure (STF), Tensile Modulus (TM), and Flexural Modulus (FM) of MBMPCs with Different Composition of LLDPE

LLDPE wt % (vol %)	TS (MPa)	STF (%)	TM (MPa)	FM (MPa)
10 (14)	0.74 ± 0.10	2.27 ± 0.31	138.83 ± 1.07	164.7 ± 5.5
15 (21)	1.38 ± 0.10	7.09 ± 0.91	398.03 ± 80.15	298.3 ± 11
20 (28)	1.98 ± 0.03	7.19 ± 2.61	475.81 ± 47.13	393.7 ± 19.3
30 (39)	2.82 ± 0.26	18.09 ± 1.56	487.08 ± 126.6	632.7 ± 23.2
40 (50)	3.99 ± 0.13	45.44 ± 6.67	450.61 ± 95.15	507.3 ± 20.6
60 (70)	6.27 ± 0.21	107.9 ± 58.93	394.34 ± 40.34	401.3 ± 13
100 (100)	31.60 ± 1.05	726 ± 32.17	281.54 ± 44.60	238 ± 16

Test samples were pre-conditioned in 50% RH at 25°C for 24 hours ( $n = 5$ ). Flexural modulus of pure MBM (0%LLDPE) was measured as  $529.1 \pm 97.3$  MPa.

Figure 4 displays the normalized tensile TS and STF of MBMPCs together with the Nielsen model predictions. The predicted values were calculated using the component volume fractions, but converted to weight fractions to facilitate comparison with experimental values on the graphs. The volume fractions needed for model calculations, were calculated using LLDPE density of 0.92 g/cc and that of MBM measured as  $1.3 \pm 0.15$  g/cc. The Nielsen models for TS of a composite, assuming no adhesion between filler and polymer matrix is displayed in eq. (1) and that for STF assuming good adhesion between filler and matrix is as in eq. (2):<sup>27</sup>

$$\sigma_c/\sigma_m \approx (1-\phi_f^{2/3})S \quad (1)$$

$$\varepsilon_c/\varepsilon_m \approx (1-\phi_f^{1/3}) \quad (2)$$

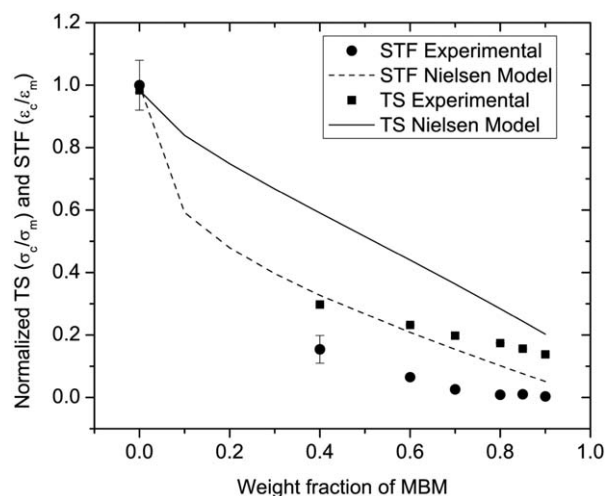
where  $\sigma_c$  is the composite TS,  $\sigma_m$  is the matrix (LLDPE) TS,  $\varepsilon_c$  is the composite strain to failure,  $\varepsilon_m$  is the matrix strain to failure,  $\phi_f$  is the volume fraction of MBM and  $S$  is a stress concentration function with a limiting value of 1 when there is no stress concentration. The function ( $S$ ) accounts for weaknesses in the structure and stress-field caused by the discontinuities at the particle/matrix interface. The STF model assumes that the polymer in the composite breaks at the same elongation as the bulk unfilled polymer.

As observed in Figure 4, the Nielsen TS model with  $S=1$  grossly over-predicts the TS of the MBMPCs. The STF model indicates that presence of small fractions of particulates rapidly decreases the STF followed by a gradual decrease. The disagreement between experimental data and model predications may be attributed to the inconsistency between the perfect adhesion assumption of the models as opposed to poor interfacial strength between MBM and LLDPE matrix. In addition, the models do not account for size and shape of the particulates, which also affect the TS and STF of composites.

MBMPCs containing LLDPE content of 15–60 wt % displayed a 40–73% larger TM compared to base LLDPE ( $282 \pm 45$  MPa). However, the composite containing 10 wt % LLDPE displayed a significantly smaller TM ( $139 \pm 1$  MPa) than that of LLDPE. Tensile moduli of MBMPCs containing 15–60 wt % LLDPE content were not statistically different from each other even

though the trend of the average TM was to increase with decreasing LLDPE content. It was observed that the flexural moduli of MBMPCs initially increased with LLDPE content of up to 30 wt % and then decreased with larger LLDPE contents of 40 wt % and above. Composites containing 30 wt % LLDPE displayed the largest FM of  $633 \pm 23$  MPa, which was more than three times that of LLDPE. Furthermore, the flexural moduli of the composites as well as pure LLDPE were found to be statistically not different from the respective tensile moduli. The smaller TM of MBMPCs containing 10 wt % LLDPE content may be attributed to the unconsolidated MBM particles observed in Figure 3 where the MBM agglomerates were not adequately encapsulated by the LLDPE phase. LLDPE content of about 15 wt % or greater was required to form a continuous LLDPE phase. Beyond that content, the flexural and TM of the composite surpasses that of the matrix.<sup>29</sup>

Figure 5 displays a comparison of the normalized TM of MBMPCs to that of the predictions by the simple rule-of-mixtures displayed in eq. (3):<sup>19,30</sup>

**Figure 4.** Normalized tensile strength (TS) and strain-to-failure (STF) of MBMPCs as a function of MBM weight fraction compared to theoretical models of Nielsen.



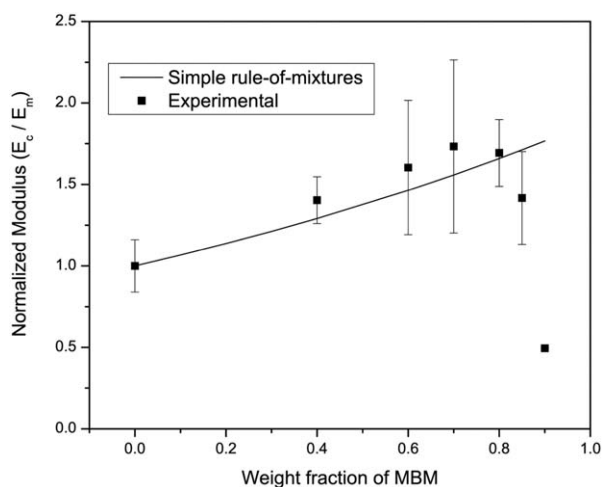


**Figure 5.** Normalized tensile modulus of MBMPCs as a function of MBM weight fraction compared to the simple rule-of-mixing model predictions.

$$\frac{E_c}{E_m} = (1 - \phi_f) + \phi_f \frac{E_f}{E_m} \quad (3)$$

Where  $E_c$ ,  $E_m$ , and  $E_f$  are the composite, matrix (LLDPE), and filler (MBM particulates) tensile moduli respectively, and  $\phi_f$  is the volume fraction of MBM. For the purpose of model prediction, the TM of MBM was assumed to be equivalent to the measured FM of 530 MPa. The simple additive model generally provided good prediction with the exception of composites containing <15 wt % LLDPE. The model works well because the modulus of MBM (530 MPa) does not vary widely from that of LLDPE (280 MPa). Also, the differential thermal shrinkage of the polymer matrix when the composite is cooled (from melt to ambient temperature) causes the polymer to mechanically bind around the MBM solid particles.<sup>23</sup> Overall, increase in the MBM content that has a larger TM than LLDPE increases the modulus of the composites until such fractions where the LLDPE does not form a continuous network, viz. at 10 wt % LLDPE content.

#### Water Vapor Permeability and Water Resistance of MBMPCs

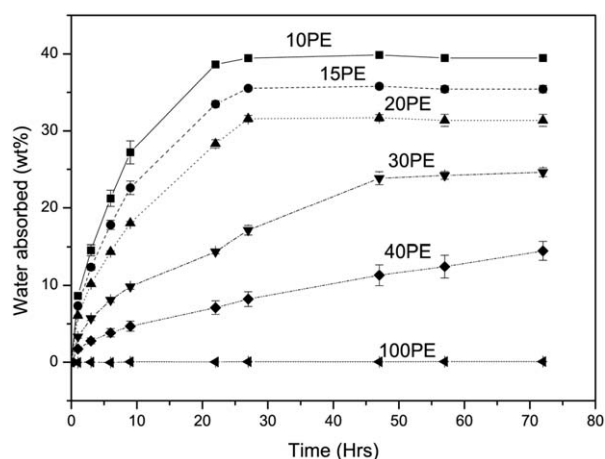
The WVP for MBMPCs containing 10, 20, 30, and 40 wt % LLDPE content was measured as  $1.34 \pm 0.20$ ,  $0.95 \pm 0.05$ ,  $0.77 \pm 0.10$ , and  $0.15 \pm 0.01$  ng/m<sup>2</sup>.s.Pa respectively. The WVP for MBM plasticized with glycerol, but containing no LLDPE, was reported as  $2.98 \pm 0.02$  ng/m<sup>2</sup>.s.Pa.<sup>4</sup> As expected, the WVP of the composites decreased with increasing LLDPE content, and was a whole order of magnitude smaller for the MBMPC containing 40 wt % LLDPE relative to that of glycerol-plasticized MBM. As the LLDPE content in the composite was increased, more MBM particles were encapsulated as observed in the SEM micrographs (Figure 3). Moreover, larger polymer content reduces voids, and thus lowers permeability of the composites. The MBMPCs still retain a hydrophilic nature as their WVP was still much larger than that of pure LLDPE ( $3 \times 10^{-5}$  ng/m<sup>2</sup>.s.Pa).<sup>28</sup>

Figure 6 displays the water absorption of MBMPCs containing 10–40 wt % LLDPE content compared to that of pure LLDPE. For each composition, mass of water absorbed gradually

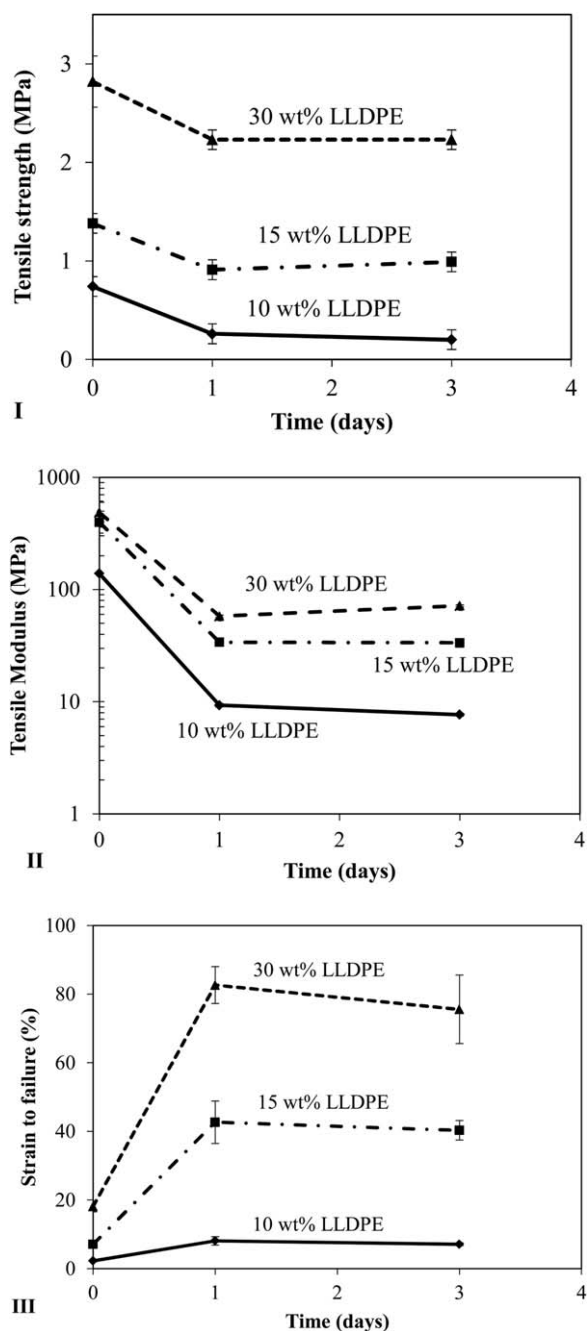
increased with time until it plateaued after about 24 hours for composites containing <30 wt % LLDPE content. As the amount of LLDPE in the composite was increased, the amount of water absorbed decreased whereas the time to reach equilibrium water concentration increased due to reduced water absorption rate. For example, the maximum amount of water absorbed by composites containing 10 and 40 wt % LLDPE was about  $39 \pm 0.1$  and  $11 \pm 1.4$  wt % after soaking for 22 and 125 hours, respectively. Therefore, consistent with the relatively higher WVP, the MBMPCs retained their hydrophilic nature such that even composites containing as much as 40 wt % LLDPE content absorbed over 10 wt % water content compared to nearly zero absorption for the pure LLDPE matrix.

Figure 7 displays the tensile properties of water-soaked MBMPCs containing 10, 15, and 30 wt % LLDPE as measured over duration of 3 days (72 hours). Both the TS and TM for all the composites decreased after one day of soaking, but remained about the same on day three. The TS of MBMPCs containing 10, 15, and 30 wt % LLDPE content decreased to  $0.7 \pm 0.1$ ,  $1.4 \pm 0.1$ , and  $2.8 \pm 0.3$  MPa, whereas the TM sharply decreased by over an order of magnitude to  $9 \pm 1$ ,  $34 \pm 3$ , and  $65 \pm 10$  MPa, respectively. In contrast, the STF of those composites increased several fold to  $8 \pm 1$ ,  $43 \pm 6$ , and  $83 \pm 5\%$  after being soaked in water for one day, and thereafter remained fairly constant. The observed trend of tensile properties changing after day one and thereafter equilibrating are consistent with the observed pattern of water absorption of MBMPCs containing LLDPE contents of 10–30 wt % displayed in Figure 6.

The decrease in the TS and TM as well as increase in the STF of the composites is due to water absorption by hydrophilic MBM in the composites. In addition, some components of MBM not encapsulated by LLDPE diffuse out of the matrix, which causes additional void formation in the structure and leads to a decrease in composite TS. This is consistent with prior observations where MBM plastic sheets processed with glycerol showed a drastic decrease in TS and TM when they



**Figure 6.** Water absorption of MBMPCs containing different contents of LLDPE (PE) as a function of time. Lines are drawn for visual comparison purpose only.



**Figure 7.** Plots showing tensile properties of MBMPCs soaked in water as a function of time: (I) tensile strength, (II) tensile modulus, and (III) strain to failure.

were exposed to high humidity conditions.<sup>3,4</sup> However, it is important to note that although MBMPCs displayed a decrease in TS and TM, the overall sample integrity was maintained, especially in samples containing 15 wt % and greater LLDPE content. In contrast, pure MBM sheets disintegrate in less than an hour as was reported in previous studies.<sup>3,4</sup> Therefore, the use of LLDPE as a binder leads to MBMPCs with good water permeability and environment stability that is important in potential semi-durable geo-structural applications such as silt-fencing.

## CONCLUSIONS

MBM animal co-product was calendered into bio-based composite sheets with LLDPE serving as a binder. Analysis of water-soaked specimens showed that a minimum of 15 wt % LLDPE content was required to form a nominally continuous matrix phase, for composites with good processability and good environmental stability. These sheets retained a TS of  $1 \pm 0.1$  MPa, a TM of  $34 \pm 3$  MPa and a STF of  $40 \pm 3$  % after being soaked in water for three days. As evidenced from WVP and water absorption measurements, MBMPCs displayed enhanced water resistance when compared with pure MBM bioplastics. Because of the enhanced water stability of these composites, relative to pure MBM, they have potential use in semi-durable geo-structural applications where water permeation and limited stability are of importance.

## ACKNOWLEDGMENTS

Financial support from Fats and Proteins Research Foundation through Animal Co-products Research and Education Center is acknowledged. This work made use of ERC Shared Facilities supported by the National Science Foundation under Award Number EEC-9731680.

## REFERENCES

- Bimbo, A. P. In *Bailey's Industrial Oil and Fat Products*; Shahidi, F. Ed.; John Wiley & Sons: New York, USA, **2005**; Vol. 57, p 62.
- Meeker, D. L. *Essential Rendering*; Kirby Lithographic Company, Inc.: Arlington, Virginia USA, **2006**, 302.
- Lukubira, S.; Ogale, A. A. *J. Appl. Polym. Sci.* **2013**, *130*, 256.
- Lukubira, S.; Ogale, A. A. ANTEC 2011: Annual Technical Conference Proceedings May 2011, Boston, MA; Society of Plastic Engineers.
- Krochta, J. M. In *Protein-Based Films and Coatings*; Gennadios, A., Ed.; CRC Press: New York, USA, **2002**; p. 1–32.
- Wool, R. P.; Sun, X. S. In *Bio-Based Polymers and Composites*; Academic Press: New York, USA, **2005**.
- Hull, D.; Clyne, T. W. *An Introduction to Composite Materials*; Cambridge University Press: New Delhi, **1996**.
- Zeller, M. A.; Hunt, R.; Sharma, S. *J. Appl. Polym. Sci.* **2013**, *127*, 375.
- Luyima, A.; Zhang, L.; Damoah, L. *JOM* **2011**, *63*, 33.
- Nikvash, N.; Kraft, R.; Kharazipour, A.; Euring, M. *Eur. J. Wood Wood Prod.* **2010**, *68*, 323.
- Ndazi, B.; Tesha, J.; Bisanda, E. *J. Mater. Sci.* **2006**, *41*, 6984.
- Jeremy Martin Warnes. U.S. Patent 20090264560A1 October 22, **2009**.
- Verbeek, C. J. R.; Pickering, K. L. *J. Reinforced Plast. Comp.* **2007**, *26*, 1607.
- Toro, P.; Quijada, R.; Yazdani-Pedram, M.; Arias, J. L. *Mater. Lett.* **2007**, *61*, 4347.
- Li, H.; Tan, Y.; Zhang, L.; Zhang, Y.; Song, Y.; Ye, Y.; Xia, M. *J. Hazard Mater.* **2012**, *217*, 256.

16. Barone, J. R.; Schmidt, W. F. *Comp. Sci. Technol.* **2005**, *65*, 173.
17. Bernice Nzioki M. Biodegradable Polymer Blends and Composites from Proteins produced by Animal Co-products Industry, Master of Science in Materials Science and Engineering, Clemson University, **2010**.
18. McGenity, P. M.; Hooper, J. J.; Paynter, C. D.; Riley, A. M.; Nutbeem, C.; Elton, N. J.; Adams, J. M. *Polymer* **1992**, *33*, 5215.
19. Fu, S.; Feng, X.; Lauke, B.; Mai, Y. *Comp. Part B: Eng.* **2008**, *39*, 933.
20. Furukawa, J. *Porima Daijesuto (Polym. Dig.)* **1988**, *40*, 10.
21. Sharma, S.; Hodges, J. N.; Luzinov, I. *J. Appl. Polym. Sci.* **2008**, *110*, 459.
22. Barone, J. R.; Schmidt, W. F.; Gregoire, N. T. *J. Appl. Polym. Sci.* **2006**, *100*, 1432.
23. Boye, J. I.; Ma, C. Y.; Harwalkar, V. R. In *Food Proteins and their Applications*; Damodaran, S.; Paraf, A., Eds.; Marcel Dekker, Inc.: New York, USA, **1997**, p 25–56.
24. Wilkinson, N., Arthur; Ryan, J., Anthony. *Polymer Processing and Structure Development*; Kluwer Academic Publishers: 3300 AA Dordrecht, The Netherlands, **1998**.
25. Huneault, M. A.; Li, H. *J. Appl. Polym. Sci.* **2012**, *126*, E96.
26. Rotheron, R. N. In *Particulate-Filled Polymer Composites*, 2nd Edn; Smithers Rapra Technology: Shrewbury, UK, **2003**; p. 235–237.
27. Nielsen, L. E. *J. Appl. Polym. Sci.* **1966**, *10*, 97.
28. Staff, P. D. L. *Permeability and Other Film Properties of Plastics and Elastomers*; William Andrew Publishing/Plastics Design Library: Norwich, New York, USA, **1995**.
29. Kuo, C.; Gupta, P. K. *Acta Metallurgica et Materialia* **1995**, *43*, 397.
30. Ahmed, S.; Jones, F. R. *J. Mater. Sci.* **1990**, *25*, 4933.